J Radioanal Nucl Chem
DOI 10.1007/s10967-016-4703-y

Compartmental and dosimetric studies of anti-CD20 labeled with ^{188}Re

Barrio Kuramoto Graciela[1] · Mie Nakamura Matsuda Margareth[1] · Alberto Osso João Jr.[1]

Received: 25 August 2015

Abstract Radioimmunotherapy has the potential to deliver lethal radiation energy directly to malignant cells via targeting of radioisotope-conjugated monoclonal antibodies (MAbs) to specific antigens. Rituximab (RTX) is specifically targeted against CD20, a surface antigen expressed by B-lymphocytes. The use of ^{188}Re from a ^{188}W/^{188}Re generator system represents an alternative radionuclide for therapy. Rhenium has chemical properties similar to technetium and both can be conjugated to antibodies using similar chemistry methods. The objective of this work is to prove the usefulness of this radiopharmaceutical based on dosimetric and pharmacokinetic studies that are also required by the Brazilian Regulatory Agency.

Keywords Radioimunotherapy · Non-Hodgkin lymphoma · Anti-CD20 · ^{188}Re · Dosimetry · Compartmental analysis

Introduction

Nuclear medicine continues to represent one of the important modalities for cancer management. The demand for therapeutic nuclear medicine is expected to exhibit rapid growth owing to its effectiveness in treating the malignancies as well as due to the development of a wide array of new products [1].

The anti-CD20 (Rituximab) is a specific chimeric monoclonal antibody directed against CD20 antigen surface on B lymphocytes, used in the treatment of non-Hodgkin lymphoma (NHL). The association with beta-emitters radionuclides have shown greater therapeutic efficacy [2–4].

Actually, two radiopharmaceuticals prepared with Anti-CD20 FDA have approval for treatment of NHL: ^{131}I-AntiCD20 (Bexar®) and ^{90}Y-AntiCD20 (Zevalin®) [5]. Techniques for radiolabeling anti-CD20 have been developed with ^{188}Re [6, 7] to evaluate the clinical use of this radionuclide in particular. The radionuclides with properties more suitable for RIT are ^{188}Re, ^{90}Y e ^{131}I, while ^{177}Lu and ^{90}Y are used in therapy with peptides receptor (PRRT).

The choice of radionuclides depends on its physical characteristics as well as characteristics of the tumor, target receptor and ligant [1]. The advantage of beta particle-emitting radionuclides is the high tumor radiation dose, while maintaining normal tissue toxicity within acceptable limits [8]. Radionuclides that decays by β^- emission are the most used for therapeutic applications in clinical practice, having an appropriate range in the tissue and low linear energy transfer (LET). Radionuclides that emits particles α have a limited range in tissue (50–80 μm) and a high LET (100 keV/μm) [9]. The Auger electrons are emitted during the process of electrons capture and internal conversion, deposit large amounts of energy on subcellular dimensions, resulting in destruction of tumor cells more efficiently [10]. Radionuclides such as ^{90}Y, ^{131}I, ^{177}Lu and ^{188}Re are in varying extent of use for the treatment of cancer and metastasis (Table 1) [11–14].

The use of ^{188}Re, produced by the decay of ^{188}W ($t_{1/2}$ = 69 d), from a ^{188}W/^{188}Re generator system has represented an alternative to RIT. In addition of β^- emission for therapy, ^{188}Re also decays by γ emission (155 keV), important in the

✉ Barrio Kuramoto Graciela
gracielabarrio@gmail.com

[1] Radiopharmacy Center, Instituto de Pesquisas Energeticas e Nucleares, Av. Professor Lineu Prestes, 2242, Cidade Universitaria, Sao Paulo, SP 05508-000, Brazil

Published online: 19 January 2016

Table 1 Nuclear characteristics from main β^- radionuclides suitable for therapy [15–17]

Nuclear characteristics	^{90}Y	^{131}I	^{177}Lu	^{188}Re
Production route	^{90}Sr/^{90}Y generator	^{235}U enriched	^{176}Lu (n, γ) ^{177}Lu	^{188}W/^{188}Re generator
Decay process	$\beta^- \rightarrow {}^{90}$Zr	$\beta^- \rightarrow {}^{131}$Xe	$\beta^- \rightarrow {}^{177}$Hf	$\beta^- \rightarrow {}^{188}$Os
Half-life	2.67 days	8.02 days	6.65 days	17.0 h
$E_{máx}$ β^- (abundance)	2.28 MeV β^- (100 %)	606 keV (90 %)	176 keV (12 %)	2.12 MeV (85 %)
			384 keV (9 %)	
			497 keV (79 %)	
Emission γ (abundance)	–	284 keV (6.1 %)	113 keV (12 %)	155 keV (15 %)
		364 keV (81.2 %)	208 keV (11 %)	
		637 keV (7.3 %)		

evaluation of biodistribution studies in vivo using gamma-camaras [18, 19] and dosimetry before the treatment. In terms of chemical properties, Re is located below technetium in periodic table. Thus, both may be conjugated to antibodies using similar chemical methods [20].

The present work aims to evaluate the effectiveness of ^{188}Re-anti-CD20 in relation to its pharmacokinetic and dosimetry, based specifically on biodistribution data extracted from literature studies [5, 7, 21, 22]. No experiments on animals were carried out in the present work. The pharmacokinetic studies were performed using a compartmental model and the dosimetric studies were performed from the study and development of animal models combined with mathematical simulations.

The compartmental model used in this work describes the metabolism of the radiopharmaceutical within the body represented by a mamilar model that consists of a central compartment, represented by blood and eleven peripheral compartments (heart, lungs, thyroid, spleen, liver, kidney, intestine, stomach, bladder, bone marrow and tumor) [23–26].

For the analysis and simulation of data obtained from biodistribution studies in literature review, the MONOLIX software was employed, that consists in using nonlinear mixed effect models with a reference platform for modeling of new drugs. MONOLIX implements a stochastic approach (SA) of expectation maximization (EM) (=SAEM) of algorithm for nonlinear mixed effect models, without approximations. The algorithm replaces the usual EM by a stochastic process more efficient with more convergence for maximum likelihood (ML) estimates. SAEM run without any approximation of the statistical model. Thus, the statistical properties "great" (consistency and minimum variance of the estimate) are expected to SAEM. The implementation of the SAEM in MONOLIX is optimized and Markov Chain Monte Carlo (MCMC) are used to define the steps of the simulation [27–31].

Experimental

^{188}Re-anti-CD20 compartmental modeling for pharmacokinetic

The pharmacokinetic study was performed with ^{188}Re-anti-CD20 radiopharmaceutical compared together with ^{131}I-anti-CD20 and ^{177}Lu-anti-CD20. A study was conducted with the α emitter ^{211}At-anti-CD20 and with the gamma emitter ^{99m}Tc-anti-CD20, where according to literature biodistribution studies, have shown satisfactory results of Anti-CD20 labeling. The evaluation of the pharmacokinetic of the radiopharmaceuticals was assessed by defining a compartmental model for the antibody. All values presented in this work for biodistribution studies were extracted from published studies [5, 7, 21, 22].

The software [27] allowed the evaluation of the pharmacokinetic behavior in the mouse body for the ^{188}Re-antiCD20 in comparison to the others products labeled with the same antibody such as ^{177}Lu, ^{131}I, ^{99m}Tc and ^{211}At.

Mathematical model of a mouse for ^{188}Re-anti-CD20

In the two methodologies proposed for calculating the absorbed dose simulated in the organs and the mouse body, a mathematical model of a mouse, was used in this work, that consists of combination of simple geometric shapes for construction of whole body, organs and tumor, where through the defined geometry for each animal organ, one can build it and use it in the necessary calculations. The mathematical equations for each organ were based on the specific dimensions of a tumor mouse about 25.0 g (nude line), with defined mass and density of the main organs values [32].

The tumor was positioned inside the mouse body, in a fixed position, near the region on the flanks. The tumor spherical shape was defined by the equation $(x + 0.5)^2 + (y - 0.7)^2 + (z - 4.5)^2 \leq 1$. For both described methods,

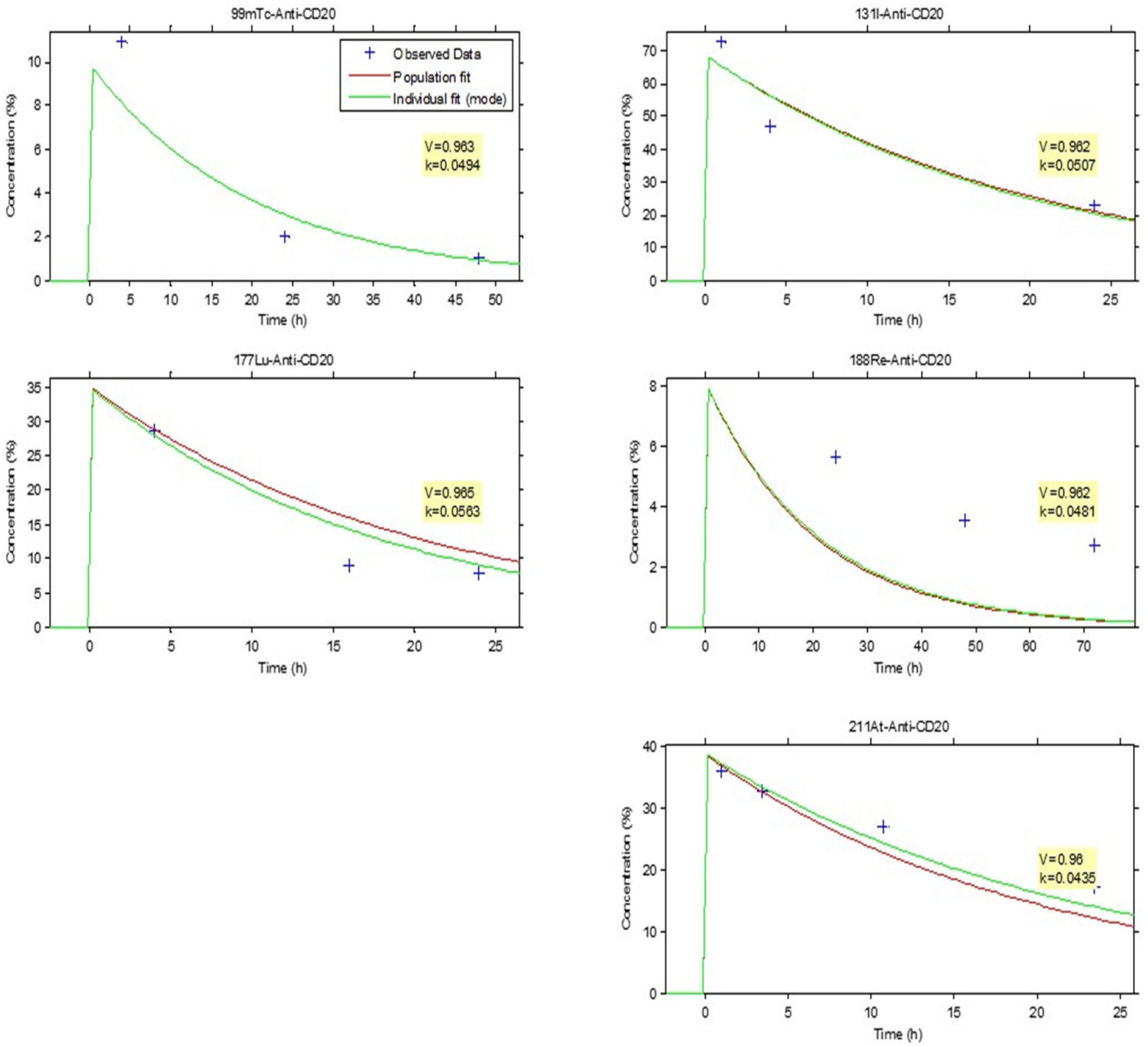

Fig. 1 Individual adjustment to the blood obtained after animal injection and biodistribution studies with ^{188}Re-Anti-CD20 compared to the labeling of the same antibody with the other radionuclides [5, 7, 21, 22]

simulations were performed where the font size (or tumor) was varied, inside the mouse body. Its radius was varied and the assessed values were 0.01–0.4 cm.

The density distribution for each organ and tumor was also defined to be uniform and was set to 1.00 g cm^{-3}, except for the lungs and the spine, for which 0.3 and 1.4 g cm^{-3} were used, respectively.

Monte Carlo simulation and point source method for ^{188}Re-anti-CD20 dosimetry

The dosimetric evaluation was performed using the Monte Carlo MCNP-4C package (Oak Ridge National Laboratory), considering ^{188}Re-anti-CD20 uniformly distributed in a spheroid as tumor mass. The simulations were carried out during 1.8×10^4 s of CPU time. The considered energy range was 1–10 MeV. This ensures reasonable uncertainties for dose distributions, generally below 1 % for all regions. The code allows the users to write their own simulation program, with arbitrary geometry and scoring. The F_8 tally gives the energy deposition in MeV at each point of the tumor. A particle source is specified by intensity, energy, direction, shape and temporal characteristics; its needs to be positioned somewhere within the phase space of the problem. The parameters used in the computations were: radius of the tumor, point of interest

Table 2 Distribution of the dose rates provided by 85 Bq of ^{188}Re-anti-CD20 into a tumor of a tumor mouse body

Tumor radius (cm)	Mass of the tumor (g)	Energy deposition (MeV)	Energy deposition per unit mass (MeV g^{-1})	Dose rate (Gy h^{-1})
1×10^{-2}	4×10^{-6}	7×10^{-2}	2×10^{4}	5×10^{-7}
2×10^{-2}	3×10^{-5}	2×10^{-2}	7×10^{2}	1×10^{-7}
3×10^{-2}	1×10^{-4}	3×10^{-2}	3×10^{2}	5×10^{-8}
4×10^{-2}	3×10^{-4}	4×10^{-2}	2×10^{2}	3×10^{-8}
5×10^{-2}	5×10^{-4}	5×10^{-2}	1×10^{2}	2×10^{-8}
6×10^{-2}	9×10^{-4}	6×10^{-2}	7×10^{1}	2×10^{-8}
7×10^{-2}	1×10^{-3}	8×10^{-2}	5×10^{1}	1×10^{-8}
8×10^{-2}	2×10^{-3}	9×10^{-2}	4×10^{1}	9×10^{-9}
9×10^{-2}	3×10^{-3}	1×10^{-1}	3×10^{1}	8×10^{-9}
1×10^{-2}	4×10^{-3}	5×10^{-2}	1×10^{1}	6×10^{-9}
2×10^{-2}	3×10^{-2}	2×10^{-1}	6	1×10^{-9}
3×10^{-2}	1×10^{-1}	2×10^{-1}	2	5×10^{-10}
4×10^{-2}	3×10^{-1}	3×10^{-1}	1	2×10^{-10}

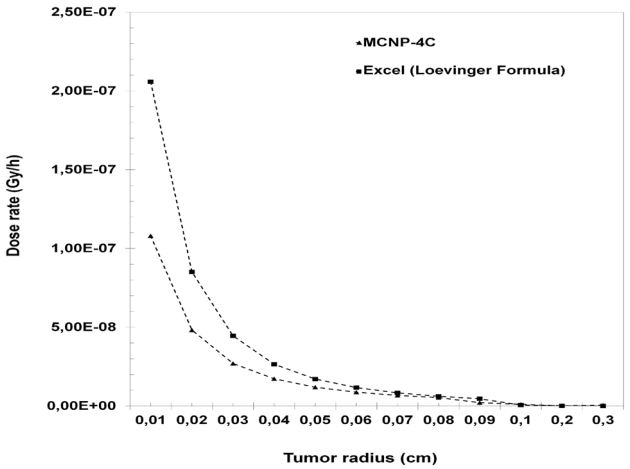

Fig. 2 Comparison of the dose rate results via analytically (by Loevinger formula) and the Monte Carlo method for ^{188}Re-Anti-CD20 in different tumor sizes, with only β^{-}particles taken into account, into the mouse body. Maximal energy: 2.12 MeV; average energy: 0.764 MeV

for dosimetry; desired dose; volume of the tumor; time since the radionuclide production; initial activity; type of the tumor; type of the radionuclide.

In order to generate the dose distribution plots in the tumor volume and surroundings, the deposited energy was integrated in spherical shell volume of constant radius.

Two different approaches were employed: on the one hand, the radionuclide was taken as uniformly distributed along the tumor mass, affecting the surrounding tissues; on the other hand, the drug intake was assumed to occur only in the tumor spherical surface. The aim of the simulation faced is to survey the real situation for the beta energies involved in this method. The method it was used too in order to evaluate the accuracy of the Loevinger formula introduced in the next section.

The Loevinger formula was used in the method that is useful for calculation of beta dose rates and different applications according to the different source geometry with β^{-} emitting radionuclides. The calculations were performed by Excel. A point source dose rate can be calculated with the Loevinger formula [33, 34]:

$$\dot{D}'[\mathrm{Gy/h}] = \frac{kA_{\mathrm{int}}}{(\mu r)^2}\left\{c\left[1-\left(\frac{\mu r}{c}\right)^{(1-\mu r/c)}\right] + \mu r e^{(1-\mu r)}\right\} \tag{1}$$

the normalization constant K it is given by:

$$k\left[\frac{\mathrm{Gy/h}}{\mathrm{Curie}}\right] = \frac{1.7 \times 10^{3}\rho^{2}\mu^{3}E_{\mathrm{av}}}{[3c^{2}-e(c^{2}-1)]} \tag{2}$$

the accumulative activity A_{int} it is given by:

$$A_{\mathrm{int}} = A_0 \cdot \left[\left(\frac{e^{-\lambda \cdot t_0}}{\lambda}\right) - \left(\frac{e^{-\lambda \cdot t}}{\lambda}\right)\right] \tag{3}$$

and the μ in air is given by:

$$\mu\left[\frac{\mathrm{cm}^2}{\mathrm{g}}\right] = \frac{16(2-E_{\mathrm{av}}/E^{*}_{\mathrm{av}})}{[E_{\mathrm{max}}-0.036)^{1.4}} \tag{4}$$

E^{*}_{av} is called the hypothetical average beta energy per disintegration for a hypothetical forbidden beta disintegration having the same E_{max} as an allowed beta decay transition in the same Z element.

We used a simple expression for beta dose rate calculation, analogy to gamma point source dosimetry, and the equation used was:

Table 3 Absorbed doses for each organ and tumor after simulations with anti-CD20 antibody labeled with ^{188}Re, compared with other radionuclides simulated in the same conditions such as ^{177}Lu, ^{131}I and ^{90}Y with MCNP, to tumors for $r = 0.04$ cm, with the distribution of radiotracer in 45 % tumor; 15 % in the heart, spleen, bladder and kidneys 10 %. Considered activity of the radiopharmaceutical: 85 Bq [7]

Absorbed dose (Gy)				
Organ	^{188}Re-anti-CD20	^{177}Lu-anti-CD20	^{131}I-anti-CD20	^{90}Y-anti-CD20
Thyroid	4×10^{1}	0	0	5×10^{1}
Heart	4×10^{2}	3×10^{2}	4×10^{2}	4×10^{2}
Liver	2×10^{1}	6×10^{-3}	3×10^{-2}	2×10^{1}
Kidneys	1×10^{2}	1×10^{2}	1×10^{2}	2×10^{2}
Spleen	4×10^{2}	3×10^{2}	3×10^{2}	4×10^{2}
Bladder	4×10^{2}	3×10^{2}	4×10^{2}	4×10^{2}
Testes	8	0	2×10^{-4}	1×10^{1}
Lungs	1×10^{2}	4	8	1×10^{2}
Column	7×10^{1}	1	3	7×10^{1}
Tumor	1×10^{3}	8×10^{2}	10×10^{2}	1×10^{3}

Table 4 Absorbed doses in tumors of different radial dimensions, calculated by the Loevinger formula

Tumor radius (cm)	Absorbed dose (Gy)			
	^{188}Re-anti-CD20	^{177}Lu-anti-CD20	^{131}I-anti-CD20	^{90}Y-anti-CD20
1×10^{-2}	9×10^{7}	6×10^{7}	7×10^{7}	10×10^{7}
2×10^{-2}	2×10^{7}	1×10^{7}	1×10^{7}	2×10^{7}
3×10^{-2}	8×10^{6}	3×10^{6}	4×10^{6}	10×10^{6}
4×10^{-2}	4×10^{6}	1×10^{6}	2×10^{6}	5×10^{6}
5×10^{-2}	2×10^{6}	5×10^{5}	8×10^{5}	3×10^{6}
6×10^{-2}	2×10^{6}	2×10^{5}	4×10^{5}	1×10^{6}
7×10^{-2}	1×10^{6}	1×10^{5}	2×10^{5}	1×10^{6}
8×10^{-2}	8×10^{5}	6×10^{4}	1×10^{5}	9×10^{5}
9×10^{-2}	6×10^{5}	3×10^{4}	8×10^{4}	7×10^{5}
1×10^{-2}	4×10^{5}	2×10^{4}	4×10^{4}	5×10^{5}
2×10^{-2}	5×10^{4}	1×10^{2}	5×10^{2}	7×10^{4}
3×10^{-2}	1×10^{4}	1	1×10^{1}	1×10^{4}
4×10^{-2}	3×10^{3}	1×10^{-2}	3×10^{-1}	4×10^{3}

$$\dot{D}_{\beta}[\mathrm{Gy/h}] = 2.14 \times 10^{4} \cdot \rho^{2} \cdot \left(\frac{\mu}{\rho}\right) \cdot A_{\mathrm{int}} E_{\mathrm{med}} \cdot \frac{e^{-\left(\frac{\mu}{\rho}\right) \cdot d \cdot \rho}}{4 \cdot \pi \cdot (d \cdot \rho)^{2}} \quad (4)$$

the ratio (μ/ρ) is given by:

$$\left(\frac{\mu}{\rho}\right)\left[\frac{\mathrm{cm}^{2}}{\mathrm{g}}\right] = 17(E_{\max})^{-1.14} \quad (5)$$

The above equations and the relation between the activity and the decay time were used in our analytical calculations of the dose rate at any desired size from the tumor in body mouse. The amounts of the radiopharmaceutical necessary for injections into mouse were so determined. The activity considered was the same determined by MCNP (the activity of the radiopharmaceutical, 85 Bq, was invariably). The composition of the tumor is important. In this work, the density of 1.00 g cm^{-3} (equal to the density of water) was used for all inner volume of the tumor.

Results and discussion

Figure 1 shows individual adjustments obtained by MONOLIX for the activity of labeled Anti-CD20 in blood, labeled with different radionuclides from different labeling methods extracted of literature: β^{-} emitters: ^{188}Re, ^{177}Lu, ^{131}I; γ emitter: ^{99m}Tc; emitter α: ^{211}At.

According to the results, the elimination rate constant k obtained for all radiopharmaceuticals was 0.05 h^{-1} that corresponds to a half-life of 14 h, inside the mouse body. For this work, the product ^{188}Re-anti-CD20 had the value of k obtained is in agreement with the values obtained for the other radionuclides. This shows its effectiveness on the anti-CD20 label process published in literature [5, 7, 21, 22].

Results of the Monte Carlo simulations and calculations with the Loevinger formula for a tumor of different sizes of radius were compared with each other. In Table 2, the results of the Monte Carlo simulation are compared with

the results of calculations by the Loevinger formula under the same conditions. The densities of the inner volume and the tumor wall were the same (1.00 g cm^{-3}). The results obtained shows a good agreement: the relative discrepancies were lower than 10 %.

The Fig. 2 shows simulations based on the main β^- spectrum (E_{max} = 2.18 MeV, 85 %) with the mean energy 0.764 MeV. According to the graph there is a correlation with dose rates obtained for the two methods, with differences of 10 % between the values obtained for each method studied for ^{188}Re-anti-CD20 simulated into a mouse body.

The Table 3 shows the absorbed doses obtained for each organ and tumor with ^{188}Re-anti-CD20 compared with the radiopharmaceuticals ^{90}Y-anti-CD20, ^{131}I-anti-CD20 and ^{177}Lu-anti-CD20, after simulations with biodistribution in tumor and organs after an injection of the product in the animal.

According to the results, it can be observed an uniform dose to the tumor for each radiopharmaceutical, with results in agreement with the input data which was initially entered to execute the code (MCNP), referring to uptake values of the main organs which are subject to a greater exposure dose (heart, spleen, bladder and the tumor itself) in an approach to a real study of in vitro biodistribution.

The Table 4 shows the absorbed dose in tumors of different radial dimensions from the Loevinger formula for point source for the radiopharmaceuticals: ^{188}Re-anti-CD20, ^{177}Lu-anti-CD20, ^{131}I-anti-CD20 and ^{90}Y-anti-CD20, through the set of mathematical equations used to construct the mouse body structure. The considered activity of the radiopharmaceutical was 85 GBq and the total time considered biodistribution was 5 h (the same activity and time performed for Monte Carlo simulation).

The results show that the bigger the size of the tumor, the lower the dose deposited and greater the chance to reach the most critical organs (such as column, kidney, liver and heart) for high energy β^- emitter. The dose behavior of radiopharmaceuticals against different tumor sizes showed the expected result, as seen by Monte Carlo simulation. Among the analyzed radiopharmaceuticals, ^{188}Re-anti-CD20 and ^{90}Y-anti-CD20 were more suitable for treating larger tumors, highlighting also the advantage of ^{188}Re have a γ energy associated, which ^{90}Y does not have, as a pure β^- emitter.

Conclusions

In The physical properties of ^{188}Re for RIT are favorable when directly labeling monoclonal antibodies. The maximum β^- emission energy of 2.12 MeV is of the same magnitude of ^{90}Y (E_{max} = 2.27 MeV), both exhibiting a similar penetrating tissue and cross-fire radiation in larger tumors by tumor cells that are not linked to the radiolabeled MAb.

The pharmacokinetic analysis performed showed that the labeling method currently for ^{188}Re-anti-CD20 is favorable, with a concordance in the results compared to other radionuclides with the same antibody.

The results obtained with the Loevinger analytical expression agree well with the results of Monte Carlo simulations with the MCNP-4C code. Effects of the half-life and mean energy of the radionuclide on the activity required for injection were studied, too. According the results, ^{188}Re-anti-CD20 was the better candidate in relation to ^{90}Y-anti-CD20, ^{131}I-anti-CD20 and ^{177}Lu-anti-CD20, for the radioimunotherapy of NHL tumors.

Acknowledgments The authors would like to thank CNEN (Comissão Nacional Energia Nuclear–CNEN/Brazil) for granting a fellowship for this work.

References

1. Das T, Pillai MRA (2014) Options to meet the future global demand of radionuclides for radionuclide therapy. Nucl Med Biol 40(1):23–32
2. Davis TA, Kaminski MS, Leonard JP, Hsu FJ, Wilkinson M, Zelenetz A, Wahl RL, Kroll S, Coleman M, Goris M, Levy R, Knox SJ (2004) The radioisotope contributes significantly to the activity of radioimmunotherapy. Clin Cancer Res 10:7792–7798
3. Kaminski MS (2005) ^{131}I-Tositumomab therapy as initial treatment for follicular lymphoma. N Engl J Med 352:441–450
4. Witzig TE, Flinn IW, Gordon LI, Emmanouilides C, Czuczman MS, Saleh MN, Cripe L, Wiseman G, Olejnik T, Multani PS, White CA (2002) Treatment with ibritumomab tiuxetan radioimmunotherapy in patients with rituximab-refractory follicular non-Hodgkin's lymphoma. J Clin Oncol 20(15):3262–3269
5. Audicio PF, Castellano G, Tassano MR, Rezzano ME, Fernandez M, Riva E, Robles A, Cabral P, Balter H, Olivier P (2011) [^{177}-Lu]DOTA-anti-CD20: labeling and pre-clinical studies. Appl Radiat Isot 69:924–928
6. Ferro-Flores G, de Murphy CA (2008) Pharmacokinetics and dosimetry of ^{188}Re-pharmaceuticals. Adv Drug Deliv Rev 60:1389–1401
7. Dias CRBR, Jeger S, Osso JA Jr, Müller C, Pasquale CD, Hohn A, Waibel R, Schibli R (2011) Radiolabeling of rituximab with ^{188}Re and ^{99m}Tc using the tricarbonyl Technology. Nucl Med Biol 38:19–28
8. Buchsbaum DJ (2000) Experimental radioimmunotherapy. Sem Radiat Oncol 10:156–167
9. Liu A, Williams L, Lopatin G, Yamauchi D, Wong J, Raubitschek A (1999) A radionuclide therapy treatment planning and dose estimation system. J Nucl Med 40:1151–1153
10. Volkert WA, Hoffman TJ (1999) Therapeutic raiopharmaceuticals. Chem Rev 99:2269–2292
11. Volkert WA, Goeckler WF, Ehrhardt GJ, Ketring AR (1991) Therapeutic radionuclides: production and decay property considerations. J Nucl Med 32:174–185
12. Srivastava SC (1996) Therapeutic radionuclides: making the right choice. In: Mather SJ (ed) Current direction in radiopharmaceutical

research and development. Kluver Academic Publishers, Dordrecht, pp 63–79
13. Srivastava SC (1999) Traditional and new isotopes for radioimmunotherapy. In: Riva P (ed) Therapy of malignancies with radioconjugates monoclonal antibodies: present possibilities and future perspectives. Harwood Academic Publishers, Chur. Switzerland, pp 11–26
14. Neves M, Kling A, Oliveira A (2005) Radionuclides for therapy and suggestion of new candidates. J Radioanal Nucl Chem 266:377–384
15. Hall DA (2011) Trivalent metals and thallium. Sampson's Textbook of Radiopharmacy. 4o Ed. 125-139
16. Cooper M (2011) Radiohalogenation. Sampson's Textbook of Radiopharmacy. 4o Ed. 141-155
17. Osso J, Knapp R (2011) Principles and Operation of Radionuclide Generators. Sampson's Textbook of Radiopharmacy. 4o Ed
18. Silverman DH, Delpassand ES, Torabi F, Goy A, Mclaughlin P, Murray JL (2004) Radiollabeled antibody therapy in non-Hodgkin's lymphoma: radiation protection, isotope comparisons and quality of life issues. Cancer Treat Rev 30:165–172
19. Milenic DE, Brechbiel MW (2004) Targeting of radio-isotopoes for cancer therapy. Can Biol Ther 3:361–370
20. Iznaga-Escobar N (1998) ^{188}Re-directed labeling of monoclonal antibodies for radioimmunotherapy of solid tumors: biodistribution, normal organ dosimetry and toxicology. Nucl Med Biol 25:441–447
21. Akanji AG (2006) Estudo de marcação com iodo-131 de anticorpo monoclonal anti-CD20 usado na terapia de linfoma não-Hodgkin's. (Master Dissertation)
22. Aurlien E, Larsen RH, Kvalheim G, Bruland OS (2000) Demonstration of highly specific toxicity of the α-emitting radioimmunoconjugate ^{211}At-rituximab against non-Hodgkin's lymphoma cells. Br J Cancer 83(10):1375–1379
23. Keith M, Norwich KH, Wong W, Jeejeebhoy KN (2000) The tissue distribution of tumor necrosis factor-a in rats: a compartmental model. Metabolism 49(10):1309–1317
24. Resigno A (2001) The rise and fall of compartmental analysis. Pharmacol Res 44(4):335–340
25. Wenger Y, Schneider RJ II, Reddy GR, Kopelman R, Jolliet O, Philbert MA (2011) Tissue distribution and pharmacokinetics of stable polyacrylamide nanoparticles following intravenous injection in the rat. Toxicol App Pharmacol 251(3):181–190
26. Wastney ME, House WA (2008) Development of a compartmental model of zinc kinetics in mice. J Nutr 138(11):2148–2155
27. MONOLIX Version 4.2.2 (2013) User Guide. Lixoft
28. Chan PLS, Jacqmin P, Lavielle M, McFadyen L, Weatherley B (2011) The use of the SAEM algorithm in MONOLIX software for estimation of population pharmacokinetic-pharmacodynamic-viral dynamics parameters of maraviroc in asymptomatic HIV subjects. J Pharmacokinet Pharmacodyn 38:41–61
29. Lavielle M, Mentré F (2007) Estimation of population pharmacokinetic parameters of saquinavir in HIV patients with the MONOLIX Software. J Pharmacokinet Pharmacodyn 34(2):229–249
30. Plan EL, Maloney A, Mentré F, Karlsson MO, Bertrand J (2012) Performance comparison of various maximum likelihood nonlinear mixed-effects estimation methods for dose–response Models. AAPS J 14(3):420–432
31. Savic RM, Mentré F, Lavielle M (2011) Implementation and evaluation of the SAEM algorithm for longitudinal ordered categorical data with an illustration in pharmacokinetics-pharmacodynamics. AAPS J 13(1):44–53
32. Hindorf C, Jungberg M, Strand SE (2004) Evaluation of parameters influencing S values in mouse dosimetry. J Nucl Med 45:1960–1965
33. Loevinger R (1954) The dosimetry of β radiations. Radiology 62:74
34. Loevinger R, Japha EM, Brownell GL (1956) Discrete radioisotope sources. I. Beta-radiation. In: Hine GJ, Brownell GL (eds) Radiation dosimetry. Academic, New York, pp 694–754